Journal of Metals, Materials and Minerals, Vol. 32, No. 1, pp. 27-40, 2022

Bio-composite of nipa palm husk derived activated carbon/poly(butylene succinate): an effective agricultural waste based adsorbent for ammonia removal

Chaichana PIYAMAWADEE[1], Viboon SRICHAROENCHAIKUL[2], and Duangdao AHT-ONG[1,3,*]

[1] *Department of Materials Science, Faculty of Science, Chulalongkorn University, Bangkok, 10330, Thailand*
[2] *Department of Environmental Engineering, Faculty of Engineering, Chulalongkorn University, Bangkok, 10330, Thailand*
[3] *Center of Excellence on Petrochemical and Materials Technology, Chulalongkorn University, Bangkok, 10330, Thailand*

***Corresponding author e-mail:** duangdao.a@chula.ac.th

Received date:
6 September 2021
Revised date
31 January 2022
Accepted date:
8 February 2022

Keywords:
Biodegradable polymer;
Activated carbon;
Nipa palm husk;
Poly(butylene succinate);
Ammonia adsorption

Abstract

In this work, activated materials were successfully prepared by pyrolyzing various ratios of Nipa palm husk powder to potassium hydroxide (1:1, 1:2, and 1:3) at predetermined temperatures (500°C, 600°C, and 700°C). The surface area was obtained from nitrogen isotherms using the Brunauer-Emmett-Teller (BET) equation. The surface area of the prepared activated carbon was increased with decreasing potassium hydroxide impregnation ratio and increasing pyrolyzing temperature. The highest surface area was 1,211 $m^2 \cdot g^{-1}$. In contrast, acidic surface functional groups investigated by Boehm's titration were increased with decreasing pyrolyzing temperature and impregnation ratio. Ammonia removal capacity was increased with an increase in the acidic surface functional groups on prepared activated carbon. Therefore, the activated sample with the highest acidic surface functional groups contents provided the greatest ammonia adsorption of around 95% (from 100 ppm to 5 ppm), implying that ammonia removal capacity was closely related to the acidic surface functional groups on the activated carbon. Adsorptive poly(butylene succinate) was carried out by incorporating activated carbon into the poly(butylene succinate) matrix for ammonia adsorption. This adsorption increased with increasing activated carbon content so that it was found that 12 wt% activated carbon provided the highest ammonia adsorption by reducing ammonia from 108 ppm to 26 ppm.

1. Introduction

Environmental pollution situations are ongoing crisis mainly due to various agriculture processes and industrial sectors, for example, farming activities, petrochemical industry, textiles industry, motor industry, and others. These industries vastly release various pollutants, including organic, inorganic, and biological substances to soil, water, and air which are both indirectly and directly harmful to human health. Extensive research has been conducted to develop effective technologies to remove or reduce these pollutants. Adsorption is considered as a promising method due to its simplicity, economic, and ease of operation. Currently, advanced adsorbent has been developed, targeting various pollutants including graphene-polypyrrole nano-particle adsorbent for Mn^{2+} removal [1], synthesized polypyrrole on polyester fabrics for copper ions removal [2], molecularly imprinted polymer (MIP) composite based porous carbon adsorbent for CO_2 capture [3], polyaniline nanofibers and nanocomposites for removal of Zn^{2+}, and Cr^{3+} removal [4].

Ammonia (NH_3) is considered an important hazardous pollutant, that it can greatly impact human health and can emit from the livestock and fertilizer manufacturing industry [5]. It is fatally poisonous to humans at elevated concentration levels of above 50 ppm to 100 ppm [6]. In addition, it irritates to the eyes, throat, and nose even at low-level concentrations. Therefore, many techniques have been developed to remove ammonia in the atmosphere, including absorption by solution, catalytic decomposition, thermal treatment as well as adsorption by porous solids [7]. The effective technique is the adsorption by porous solid using dry adsorbents due to their cost-effectiveness, simplicity, economic configuration, and operation [8]. Among dry adsorbents, activated carbon is widely used because of its high surface area, high degree of porosity, and feasibility for surface modification. It is well known that the pore structure consists of micropores, mesopores, and macropores, which are the key factors in controlling the gas adsorption ability of the materials [9]. However, the surface chemistry of activated carbon is also important for adsorptive properties, especially polar chemicals.

Surface functional groups on activated carbon can typically be divided into acidic group and basic group. Oxygen functional groups generally are acidic groups, which mainly comprise of carboxyl, phenolic hydroxyl, and lactone. They have been reported as being responsible for polar molecule adsorption such as NH_3 [10]. Kim *et al.* [11] confirmed that the total amount of polar chemical adsorbed depended on the oxygen surface group of acidic groups. Guo *et al.* [12] showed result that NH_3 removal increased with an elevated amount of acidic surface functional groups on palm-shells- activated carbon.

Activated carbon (AC) is normally prepared from carbonaceous materials such as anthracite and bituminous coals. However, at the present time, manufacturers and researchers are increasingly interested

in producing porous carbons from waste products as precursor materials [13]. This is because conventional source (from agriculture and wood industry) and non-conventional source (from municipal and industrial activities) are identified as huge carbon source. As a result, recycling different types of waste materials is logical in aspect of both added economic value to the waste and from technical standpoint. Hence, research in porous carbon preparation from recycling wastes has been carried out using, for example, viscose rayon cloth [14,15], mandarin peel [16] to prepare nanoporous carbon material. For, AC, agricultural wastes are suitable raw materials for the production of AC because they are renewable resources from nature containing high amount of cellulose, hemicellulose, and lignin, as well as being cost-effective. Furthermore, different natural biomasses being used to produce AC may show different adsorptive properties such as surface area, pore size, pore volume, and particle size [17,18]. Therefore, finding alternative raw materials from natural biomass that are low-cost and readily available has been a topic of major interest [19].

Nipa palm (*Nipa fruticans*) is a monoecious palm with special characteristics different from usual palms like coconut and oil palm. It grows fast and is available in all seasons and has a large amount of biomass. However, it has not been effectively utilized to create economic advantages [20]. Therefore, various parts of the Nipa palm have been investigated, including the frond, leaf, husk, and shell.

Poly(butylene succinate) (PBS) is biodegradable, biocompatible, and has mechanical properties similar to those polyolefins such as polyethylene commonly called a tough polymer. Furthermore, PBS can be easily fabricated to be a sheet, and filler incorporation can be conducted. Therefore, this biodegradable polymer is a promising way to prepare adsorptive polymer which has adsorption properties. Recently, the incorporation of activated carbon has been focused on the improvement of mechanical, thermal properties of PBS, but no report information has not been reported about their adsorptive properties.

This work aimed to investigate the capability of porous carbon derived from Nipa palm husk to adsorb NH_3 and to prepare a novel biodegradable polymer-based system, as potential bio-adsorptive material. Nipa palm husk was used as a precursor and subjected to an activation agent as KOH. The effects of Nipa palm husk powder to KOH (w/w), activation temperature on the textural and chemical characteristics were explored. Moreover, the relationship between NH_3 adsorption capacity and surface functional groups was also examined. Adsorptive PBS was prepared by dispersing obtained porous carbons into PBS matrix and was investigated the effect of obtained activated carbon contents on physical and thermal properties of obtained PBS. Furthermore, particular attention involving the ammonia adsorption capability of adsorptive PBS was also investigated.

2. Experimental

2.1 Materials

Nipa palm husk used as raw material was collected from Nakhon Pathom Province, Thailand. It was washed with water and dried by sunlight. Then, the raw material was crushed and sieved to a particle size of around 1 mm. The proximate analysis and ultimate analysis of this material are shown in Table 1. The chemical characteristics of Nipa palm husk showed significant potential to convert into Activated carbon (AC) because of its relatively high fixed carbon and low ash content in proximate analysis. Furthermore, the ultimate analysis showed that the carbon content was highly similar to fixed carbon. The amount of oxygen was 43.29 wt%, which could be expected to become surface functional groups on AC surface.

Poly(butylene succinate) (PBS) (BioPBS, Grade FZ91PM) with MFI 5 g·10 min^{-1} (199°C, 2.16 kg) was purchased from PTT MCC Biochem Company Limited (Thailand).

Potassium hydroxide (KOH) and Sodium carbonate (Na_2CO_3) (AR grade) were supplied by Thermo Fisher Scientific Ltd., Auckland, New Zealand. Sodium hydroxide (NaOH) (AR grade) was purchased from RCI Labscan Ltd., Bangkok, Thailand. Sodium bicarbonate ($NaHCO_3$) (AR grade) was obtained from BDH Chemicals Ltd., Dubai, UAE. Sulfuric acid (H_2SO_4) (95% to 98%) was supplied by Sigma-Aldrich Pte. Ltd., Singapore. Ammonia (NH_3) solution (28%, AR grade) was supplied by Qrec (Asia) Ltd., Selangor, Malaysia.

2.2 Preparation of Nipa palm activated carbon

Nipa palm husk powder was mixed with KOH solution (analytical grade, Ajax finechem) at various impregnation ratios (palm husk powder to KOH weight ratios of 1:1, 1:2, and 1:3) and then evaporated at 110°C for 24 h. Each impregnated sample was then activated using a horizontal fixed-bed reactor for 1 h at various activation temperatures with 10°C·min^{-1} heating rate under Nitrogen (N_2) gas flow of 100 mL·min^{-1} to achieve activated carbon. The experimental setup was adapted from Sricharoenchaikul *et al.* [21]. The activation temperature was varied from 500°C to 700°C. Finally, the obtained activated carbon was washed with distilled water until attaining constant pH and dried at under 105°C for 24 h, then stored in a desiccator. The nomenclature for the obtained activated carbon (ACX_Y) was the AC followed by impregnation ratio (X) and activation temperature (Y).

Proximate analysis for characterizing fixed carbon, moisture, volatile matter, and ash was carried out following ASTM D121, while ultimate analysis to determine carbon, hydrogen, nitrogen, and oxygen contents were performed by CHN analyzer (Flash2000, Thermo scientific).

Table 1. Proximate and ultimate analysis of Nipa palm husk.

Proximate analysis (wt%)		**Ultimate analysis (wt%)**	
Fixed carbon	40.50	Carbon	50.23
Volatile	52.23	Hydrogen	8.02
Ash	2.72	Nitrogen	0
Moisture	4.24	Oxygen[a]	41.75

[a] Oxygen was calculated by difference

2.3 Preparation of adsorptive PBS sheet

The preparation of the adsorptive PBS sheet was carried out by mixing PBS pellets and activated carbon, using four different compositions (3 wt%, 6 wt%, 9 wt%, and 12 wt% AC). PBS and activated carbon were dried in the air-circulating oven at 60°C for 24 h to eliminate moisture. 1 kg of PBS was mixed with a predetermined amount of AC to provide the exact concentration. The mixture of PBS and AC was thoroughly shaken until seeing homogeneous mixture by naked eyes and then compounded by the melting process in a twin screw extruder (LTE-26-44, Labtech Engineering Co., Ltd., Thailand). The temperature profiles of twin screw extruder were in the range of 130°C to 170°C with a screw speed of 40 rpm. The extrudate was cooled in a water bath and then pelletized in granulated form. The adsorptive PBS sheet was fabricated by a chill-roll cast film extrusion (LCR-300 Co-Ex, Labtech Engineering Co., Ltd., Samutprakarn, Thailand) using barrel temperature of 150°C to 190°C, screw speed of 45 rpm, chill roll speed of 3.5 $m \cdot min^{-1}$, and wind speed of 5.4 $m \cdot min^{-1}$. The final thickness was controlled between 240 μm to 270 μm.

2.4 Characterization of prepared activated carbon

The textural characteristics, including surface area and porous texture, were characterized using nitrogen adsorption isotherms by automated adsorption apparatus (Autosorb-1, Quantachrome, Graz, Austria). The N_2 adsorption-desorption isotherms were performed to determine these parameters including specific surface area, micropore surface area, total pore volume, and total micropore volume. The specific surface area was calculated using the Brunauer-Emmett-Teller (BET) equation [22]. Total pore volume was estimated from the amount of nitrogen adsorbed at relative pressure around 0.997. The micropore surface area and micropore volume were calculated by t-method.

Surface acidic groups were determined by Boehm's titration method [23]. First, 0.1 g of AC sample was placed in 10 mL of one of three reactants including 0.1 M NaOH, 0.1 M $NaHCO_3$, 0.05 M Na_2CO_3. The mixtures were shaken for 24 h at room temperature, after that the AC samples were filtered out. Finally, the excess acid was pipetted with 0.05 M H_2SO_4. The amount of acidic surface functional groups was calculated according to these assumptions; NaOH neutralizes carboxyl, phenolic and lactonic groups; Na_2CO_3 neutralizes carboxyl and lactonic groups, and $NaHCO_3$ only reacts with carboxyl groups. Surface acidic groups on prepared activated carbon were calculated by an equation which is modified from Boehm's titration method [23] as below:

$$\underset{(mmol/g\text{-}AC)}{Acidic\ funtional\ group\ content} = \frac{[(C_i \times 10) - (n \times C_{titrant} \times V)]}{w}$$

where C_i = 0.1 M for NaOH and $NaHCO_3$, or 0.05 M for Na_2CO_3
n = 1 for Na_2CO_3, or 2 for NaOH and $NaHCO_3$
$C_{titrant}$ = H_2SO_4 concentration ($mol \cdot L^{-1}$)
V = volume of H_2SO_4 used (mL)
w = activated carbon weight (g)

Ammonia was used as an adsorbate in the gas phase and the prepared activated carbon was employed as an adsorbent for the ammonia adsorption experiment. Ammonia solution was diluted to 2800 ppm and then partially vaporized into the gas phase for mixing with pure N_2 gas to prepare the predetermined concentration. For this experiment, 0.1 g of the activated carbon was enclosed in a plastic tube where the efficiency of porous materials to adsorb NH_3 was to be evaluated. The initial concentration of ammonia gas in the plastic tube was determined at approximately 100 ppm to 110 ppm. The entire adsorption experiment was tested at room temperature without any ambient light. NH_3 concentration was measured using a sampling system consisting of a gas-sampling pump (GV-100, GASTEC, Kanagawa, Japan) and detector tube (No. 3La, GASTEC, Kanagawa, Japan). This equipment showed that the NH_3 concentration as gas in the plastic tube was pumped into the detector tube by a gas pump. NH_3 concentration in the plastic tube was measured at 0 h, 1 h, 2 h, 13 h, and 24 h. The experimental setup is shown in Figure 1.

NH_3 equilibrium capacity on the prepared activated carbon was calculated from an equation which is adjusted from Huang *et al.* [24] as follows:

$$\underset{(mmol\text{-}NH_3/g\text{-}AC)}{NH_3\ equilibrium\ capacity} = \frac{50 \times (C_f - C_i)}{1000 \times M \times w}$$

where C_i = NH_3 inlet concentration (ppm)
C_f = NH_3 final concentration (ppm)
M = molecular weight of ammonia
w = weight of activated carbon (g)

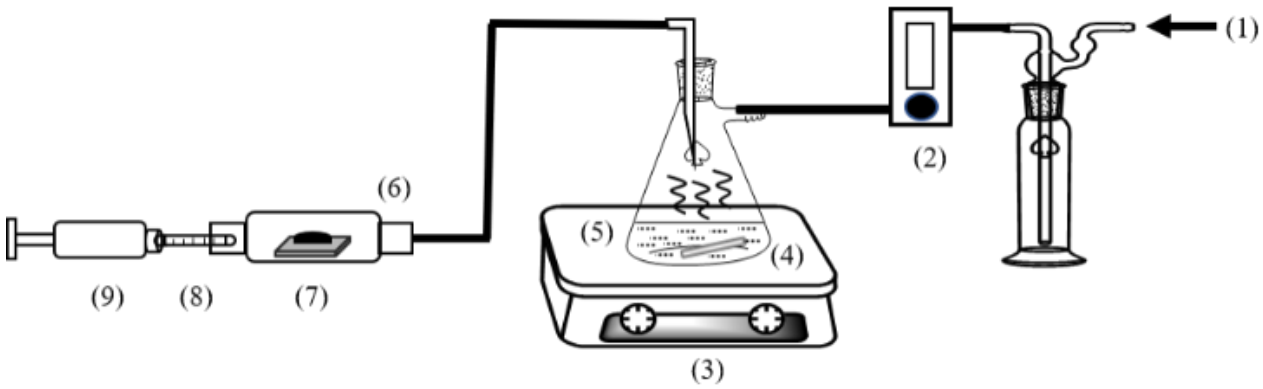

Figure 1. Experimental set up for ammonia adsorption (1) Nitrogen gas, (2) Flow controller, (3) Hot plate, (4) Magnetic bar, (5) Ammonia solution, (6) Ammonia adsorption chamber, (7) Activated carbon, (8) Detector tube, and (9) Gas sampling pump.

2.5 Characterization of adsorptive PBS sheet

Thermal properties of adsorptive PBS sheet were analyzed by Differential scanning calorimetry (DSC; TGA/DSC3+, Mettler-Toledo, Greifense, Switzerland). Approximately, 3 mg to 4 mg of sample was heated from 30°C to 200°C at a heating rate of 10°C·min^{-1} under nitrogen atmosphere for eliminating thermal history. Then, the cooling step was subsequently followed by reducing the temperature to 30°C at the same rate. Finally, the second heating was performed to 200°C at a rate of 10°C·min^{-1}. This characterization provided the output data including crystallization temperature (T_c) determined during the cooling scan, melting temperature and melting enthalpy (Δ_{Hm}) represented during the second heating scan.

Surface functional groups on adsorptive PBS sheet were characterized using Fourier transform infrared spectroscopy (Nicolet 6700, Thermo Scientific, Waltham, MA) recording wavenumber of 4000 cm^{-1} to 400 cm^{-1}. ATR mode on an adapter with a crystal ZnSe was performed for investigation of surface functional groups of PBS samples. The number of scans was 16 and the resolution was 64.

The surface morphologies of the adsorptive PBS sheet were observed through a scanning electron microscope (SEM; JSM 6480LV; JEOL, Tokyo, Japan) at an accelerating voltage of 15 kV. Before characterizing, samples were dried in an air-circulating oven at 60°C for 24 h and mounted on a stub with carbon tape. Then, a thin layer of gold was sputter-coated to the samples under vacuum condition to protect the charging of the surface under an electron beam.

Wettability of adsorptive PBS sheet was characterized by water contact angle using a contact angle meter (DM-CE1, Kyowa, Saitama, Japan). The samples were cut into the dimension of 5 cm^2 × 5 cm^2. The contact angle was estimated three times and the drop of water used had a volume of 3 µl.

Ammonia was used as an adsorbate in the gas phase and the prepared PBS sheet were employed as an adsorbent for ammonia adsorption. Ammonia solution was diluted to 2800 mg·L^{-1} and then partially vaporized into the gas phase for mixing with pure N_2 gas to prepare the predetermined concentration. 10 cm^2 × 10 cm^2 of the prepared PBS sheet was enclosed in a plastic tube where the efficiency of the sample to adsorb NH_3 was to be evaluated. The initial concentration of ammonia gas in the plastic tube was determined at 100 mg·L^{-1} to 110 mg·L^{-1} approximately. The entire adsorption experiment was tested at room temperature without any ambient light. NH_3 concentration was measured using a sampling system consisting of a gas-sampling pump (GV-100, GASTEC, Kanagawa, Japan) and detector tube (No. 3La, GASTEC, Kanagawa, Japan). This equipment showed that the NH_3 concentration as gas in the plastic tube was pumped into the detector tube by a gas pump. NH_3 concentration in the plastic tube was measured at 0 h, 1 h, 2 h, 13 h, and 24 h.

3. Results and discussion

3.1 Proximate and ultimate analysis of prepared activated carbon

The results of proximate and ultimate analysis for prepared activated carbon compared with raw material are shown in Table 2.

All samples showed higher fixed carbon content than the raw material, while volatile content of all samples was lower. The increment of the fixed carbon content for the obtained activated carbon was due to the elimination of volatile matter in the Nipa palm husk at high temperature. Furthermore, increasing activation temperature (500°C to 700°C) and KOH used (1 time to 3 time compared with raw material) helped to increase fixed carbon content, while these parameters increasingly eliminated volatile matter out of the sample. Therefore, AC13_700 which was employed the highest amount of KOH, and activation temperature obtained the highest fixed carbon of 78.6% and the lowest volatiles of 16.1%.

For, ultimate analysis, the high content of C and O elements for the husk of 50.23% and 41.75% respectively, were due to the main composition of Nipa palm husk which includes cellulose, hemicellulose, and lignin [25]. The results of elemental analysis for the obtained samples significantly depended on the effect of the impregnation ratio and activation temperature. When studying the effect of various impregnation ratios, the results shows significant a decrease in carbon content from 67.68% to 46.72% at 500°C with decreasing ratio, whereas an increase in oxygen content was obviously observed. It can be attributed that KOH mainly reacted with carbon, affecting carbon content reduction [26]. For the effect of different activation temperatures, carbon content decreased at an impregnation ratio of 1:1 with increasing activation temperature from 500°C to 700°C, while oxygen content increased significantly. This was due to the vigorous reaction of KOH on the carbon surface affecting the creation of surface functional group on the surface, which subsequently caused

Table 2. Proximate and ultimate analysis of prepared activated carbon compared with raw material.

Sample	Content (% by weight)							
	Proximate analysis				Ultimate analysis			
	Fixed carbon	Volatile	Moisture	Ash	Carbon	Hydrogen	Nitrogen	Oxygen*
Nipa palm husk	40.50	52.23	4.24	2.72	50.23	8.02	0	41.75
AC11_500	55.32	36.74	2.23	5.70	67.68	3.07	0.03	29.22
AC11_600	60.68	34.75	1.25	3.32	63.67	2.40	0.04	33.90
AC11_700	64.68	30.80	0.99	3.53	61.77	2.08	0.03	36.12
AC12_500	61.72	29.92	1.39	6.96	57.86	1.89	0.03	40.22
AC12_600	65.43	27.61	1.06	5.90	52.12	2.12	0.05	45.72
AC12_700	74.65	22.69	0.86	1.79	54.17	2.21	0.02	43.60
AC13_500	65.46	24.89	0.77	8.89	46.72	2.28	0.03	50.96
AC13_600	74.43	18.82	0.71	6.04	48.62	2.41	0.03	48.94
AC13_700	78.54	16.06	0.92	4.48	49.12	2.51	0.03	48.34

*Oxygen was calculated by difference.

an increase in oxygen content. The reaction of activation agent and surface carbon (C_s) possibly occurs during the activation process, which can be written as the following equations [27]:

$$4KOH + C_s \rightarrow K_2CO_3 + K_2O + 2H_2 \quad (1)$$

$$K_2CO_3 + 2C_s \rightarrow 2K + 3CO \quad (2)$$

$$K_2O + C_s \rightarrow C - O\text{-}K + K \quad (3)$$

$$C\text{-}O\text{-}K + H_2O \rightarrow C\text{-}O\text{-}H + KOH \quad (4)$$

At ratios of 1:2 and 1:3, oxygen content slightly decreased with increasing temperature from 500°C to 700°C. It could be that K_2O was reduced to K metal, which caused to release volatile matter instead of creating surface functional groups [27]. This suggestion agreed with the result of proximate analysis showing that volatile matter decreased with a change in activation temperature from 500°C to 700°C. Equation (5) is the reaction of K_2O with carbon surface at a large amount of KOH and high activation temperature [26].

$$K_2O + C_s \rightarrow 2K + CO \quad (5)$$

3.2 Textural analysis of prepared activated carbon

The specific surface area and pore volume of all activated carbon data were summarized in Figure 2(a-b), respectively. From Figure 2(a), it can be seen that BET surface area (S_{BET}) and micropore surface area ($S_{micropore}$) of all samples were similar, indicating that micropores highly impacted the surface area of prepared activated carbon. For the effect of activation temperature on the specific surface area of obtained activated materials at each impregnation ratio, this result shows that S_{BET} was progressively increased with reaction temperature from 500°C to 700°C. It can be demonstrated that increasing the activation temperature provoked KOH molecule penetration to the interior of the raw material, inhibiting the formation of tar and obstructing particle shrinkage [13]. In addition, decreasing the impregnation ratio (1:1 to 1:3) also improved BET surface area. This factor also enhanced the porosity development of activated carbon, as mentioned before.

However, S_{BET} and $S_{micropore}$ decreased at an impregnation ratio of 1:3 at activation temperature of 500°C and 600°C. This result may be due to greater amount of KOH, which strongly attacked carbon structure promotion over oxidation of carbon to carbon dioxide and inducing a combination of micropores, resulting in an increase of mesopores (pore diameter between 2 nm to 50 nm.). This is consistent with the results shown in Figure 2(a-3). The highest BET surface area and total pore volume obtained from activating raw material at impregnation ratio of 1:3 for 700°C were 1211 $m^2 \cdot g^{-1}$ and 0.8351 $mL \cdot g^{-1}$, respectively. Therefore, the obtained activated carbon can be introduced for utilizing on a commercial scale since practical activated carbon should generally have BET surface area greater than 500 $m^2 \cdot g^{-1}$ [28].

3.3 Morphological analysis of prepared activated carbon

Figure 3 shows SEM photographs of all AC samples. Overall, the SEM micrographs show non-uniform pores, irregular shapes on the outer surface and channels to the interior of AC, which pointed to KOH permeation resulting in the creation of new pores. This is because KOH molecules are small and fast to diffuse into the pores of AC. Consequently, KOH reaction on AC surface occurs rapidly, leading to the creation of new pores with irregular shape and size.

For each impregnation ratio, the activation temperature significantly affects the surface morphology of AC. When activation temperature was increased from 500°C to 700°C, large visible pores were clearly observed. This is attributable to higher temperature causing more volatile matter being released from raw material and higher carbon burn-off, resulting in small pore expansion to large pore.

When the effect of impregnation ratios was investigated, pore structure and the shape of pores were clearly changed by pore enlargement with decreasing ratio from 1:1 to 1:3. This change could be ascribed to a greater amount of KOH in the matrix, causing more gasification by reduction of KOH to K_2CO_3 and K_2O, as shown in Equation (1)-(3). However, more porous structure of prepared AC at an impregnation ratio of 1:3 seems to be destroyed when compares to those at 1:1 and 1:2. This is probably due to the excess amount of KOH generating more gaseous products such as water and CO_2, as shown in Equation (6). These gaseous products can cause additional gasification, leading to more pores, widening pore space and merging micropores into mesopores [29]. This phenomenon from SEM observation corresponds with BET report, in which micropore surface area proportion of AC prepared at an impregnation of 1:3 is lower than AC from other impregnation ratios.

$$2KOH \rightarrow K_2O + H_2O \quad (6a)$$

$$H_2O + C \rightarrow CO + H_2 \quad (6b)$$

3.4 Surface chemistry of prepared activated carbon

The effect of different impregnation ratios and activation temperatures on acidic surface functional groups was determined using the Boehm titration technique, as shown in Table 3. The total acidic and acidic functional groups including phenolic, carboxylic, and lactonic groups, obviously decreased with increasing activation temperature from 500°C to 700°C at the evaluated impregnation ratio. According to Van *et al*. [30], total acidic functional groups of AC prepared from rice husk impregnated with NaOH were lower with an increase of activation temperature from 650°C to 800°C. This phenomenon can be ascribed from the thermal decomposition of acidic groups around 100°C to 650°C [31]. Therefore, the highest activation temperature of 700°C provided the lowest amount of acidic functional group for each ratio.

On the contrary, the acidic functional groups were linearly dependent on activating agent content used in the reaction according to the results from Table 3. This is due to a great amount of KOH being more reactive with the surface of activated carbon during the activation process, resulting in the creation of new acidic functional groups. Among these acidic groups, phenolic functional group is the most sensitive with reaction temperature as it rapidly decreased with increasing activation temperature, whereas the lactonic functional group was quite stable. This result corresponds to other researchers'works. Mochizuki *et al*. [32] studied the influence of KOH on the surface chemistry of obtained activated carbon prepared from petcoke. They observed that phenolic hydroxyl significantly decreased with increasing activation temperature from 600°C to 800°C.

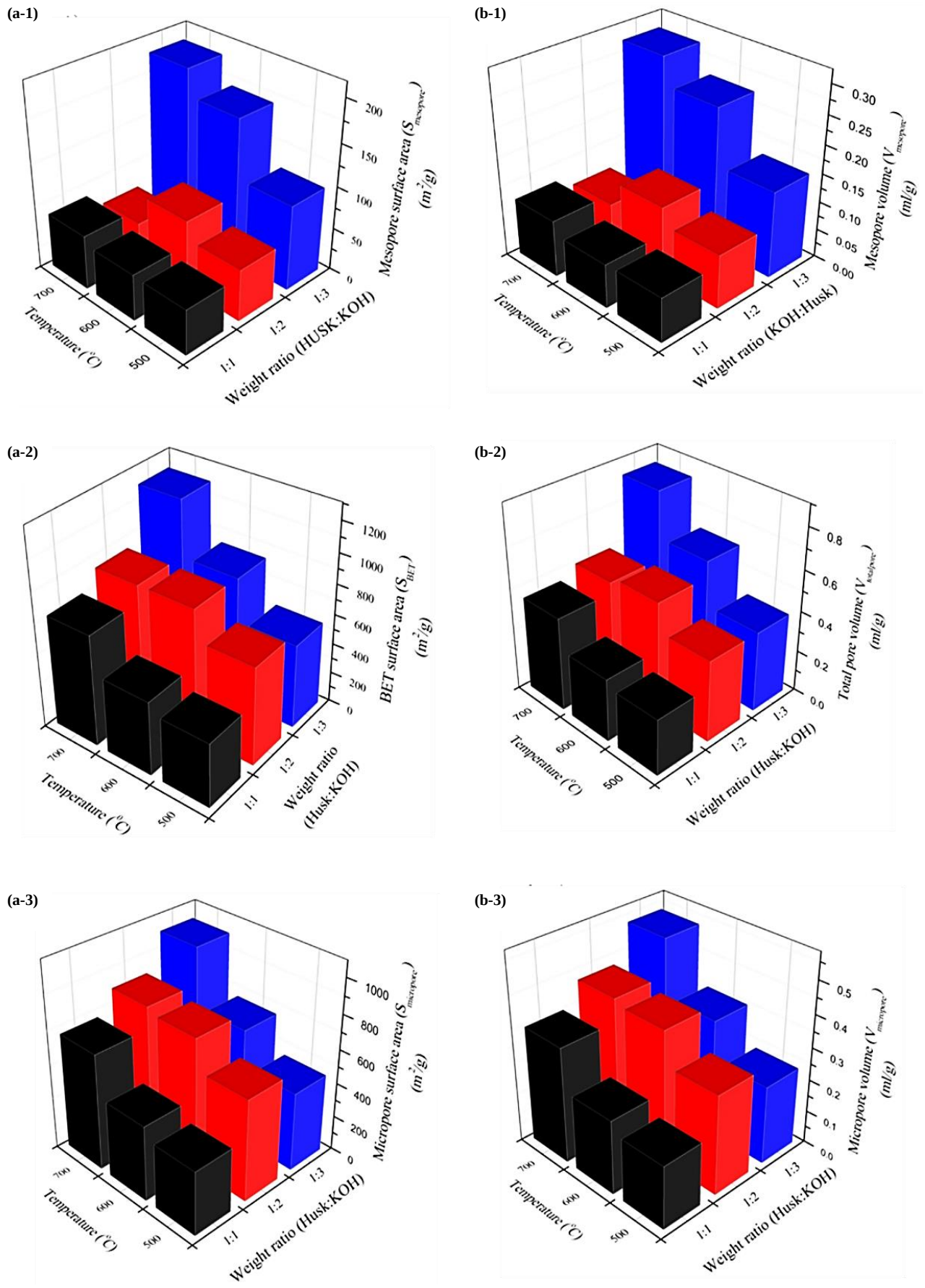

Figure 2. Effect of impregnation ratio and activation temperature on (a-1) mesopore surface area, (a-2) BET surface area, (a-3) micropore surface area, (b-1) mesopore volume, (b-2) total pore volume, and (b-3) micropore volume of obtained activated carbon.

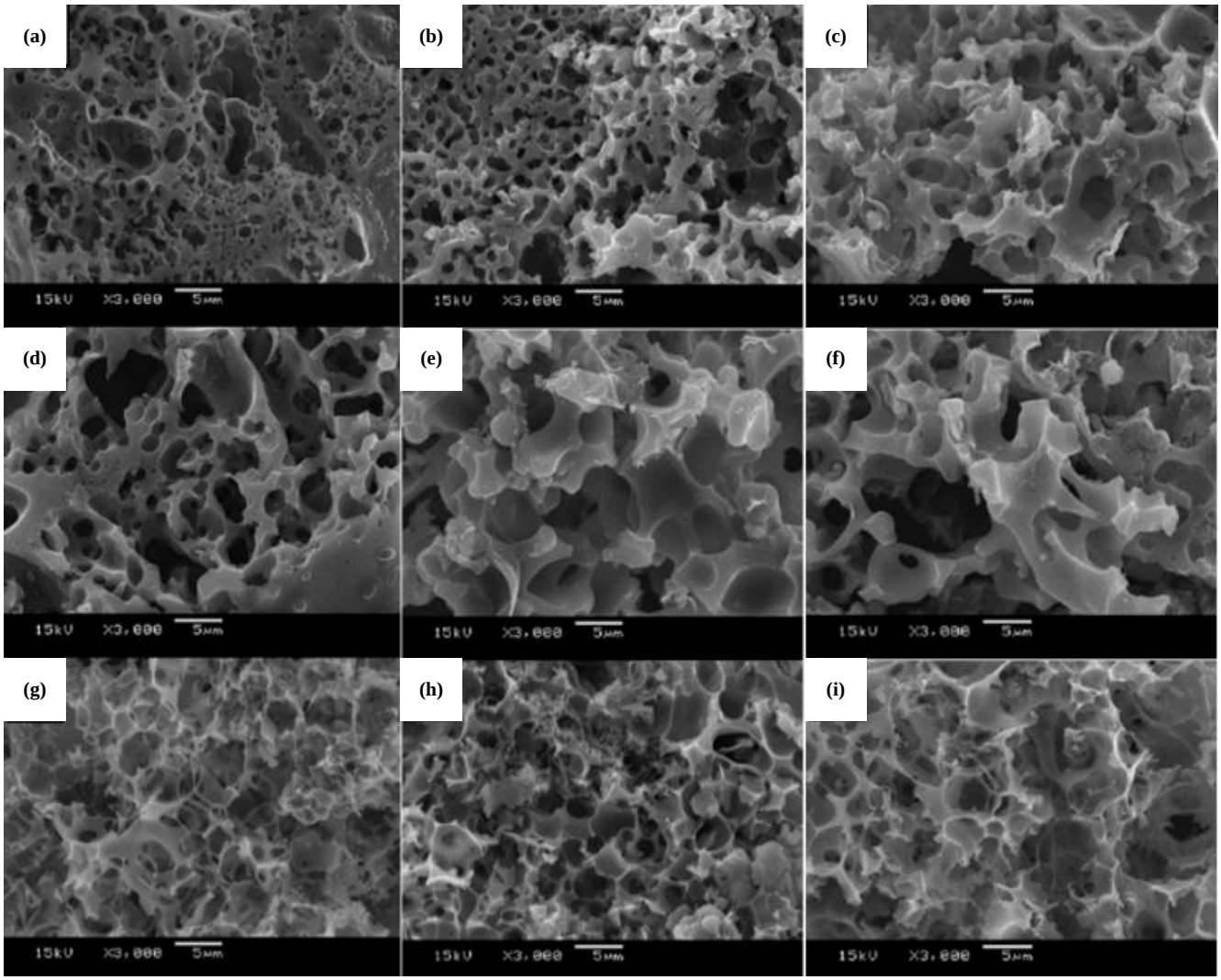

Figure 3. Scanning electron micrographs of (a) AC11_500, (b) AC11_600, (c) AC11_700, (d) AC12_500, (e) AC12_600, (f) AC12_700, (g) AC13_500, (h) AC13_600, and (i) AC13_700.

Table 3. Acidic surface characteristics of activated carbon prepared by using different impregnation ratios and activation temperatures.

Sample	Acidic functional groups content (mmol/g-AC)		
	Phenolic group	**Lactonic group**	**Carboxylic group**
AC11_500	1.28	0.22	3.51
AC11_600	0.50	0.20	3.82
AC11_700	0.32	0.15	3.05
AC12_500	1.33	0.44	4.36
AC12_600	0.93	0.38	3.75
AC12_700	0.46	0.35	3.68
AC13_500	1.51	0.46	5.01
AC13_600	0.91	0.42	4.14
AC13_700	0.38	0.36	3.76

3.5 Ammonia adsorption efficiency of prepared activated carbon

Table 4 shows the NH_3 residues, this gas was rapidly adsorbed within 1 h to 2 h followed by slow removal until reaching an equilibrium state. This result shows that the activated sample from the impregnation ratio of 1:3 at activation temperature of 500°C can reduce ammonia in the system around 95% (from 100 ppm to 5 ppm). Furthermore, there is an indication of the high capability of prepared ACs on NH_3 removal and their capacity inducing equilibrium within 24 h. The ammonia adsorption efficiency of each sample can be directly indicated from NH_3 equilibrium capacity as shown in Table 5 so that it can be concluded that the highest and lowest effective adsorption for obtained samples are AC13_500 and AC11_700, respectively.

Table 4. Removal efficiencies for NH_3 adsorbed on AC prepared by different impregnation ratios and activation temperatures.

Sample	NH_3 content residue (%)				
	0 h	1 h	2 h	13 h	24 h
AC11_500	100	31.32	22.89	18.07	16.87
AC11_600	100	41.77	36.71	17.72	17.72
AC11_700	100	53.22	49.32	45.76	43.58
AC12_500	100	27.91	18.60	15.12	13.95
AC12_600	100	43.75	32.5	17.5	15
AC12_700	100	46.81	44.68	34.04	36.17
AC13_500	100	17.65	10.59	4.12	4.71
AC13_600	100	25.81	17.20	6.45	9.68
AC13_700	100	53.85	38.46	22.46	23.08

Table 5. BET surface area and total acidic groups of prepared AC on NH_3 equilibrium capacity.

Samples	BET surface area ($m^2 \cdot g^{-1}$)	Total acidic groups (mmol/g-AC)	NH_3 equilibrium capacity (mmol-NH_3/g-AC)
AC11_500	426	5.00	2.44
AC11_600	491	4.50	2.49
AC11_700	739	3.88	2.26
AC12_500	651	6.08	2.65
AC12_600	852	5.01	2.50
AC12_700	848	4.41	1.93
AC13_500	558	6.98	2.94
AC13_600	840	5.42	2.65
AC13_700	1211	4.44	1.79

The effect of acidic surface groups and textural characteristics represented as BET surface area on ammonia adsorption was investigated. BET surface area shows no relationship with NH_3 equilibrium capacity, indicating that it is independent of the textural characteristics. Meanwhile, total acidic groups content seems to have a linear relationship with NH_3 adsorption capacity. So, finding the relationship between NH_3 equilibrium capacity and acidic groups content was be conducted and displayed result in Figure 4, where the coefficient of determination (R^2) was generally taken to measure how closely the data was fitted to the regression line.

This figure shows that the coefficient of determination for carboxylic ($R^2 = 0.4381$) and phenolic group ($R^2 = 0.5563$) has a close relationship with that of total acidic groups ($R^2 = 0.5562$). Interestingly, this means that both groups in the prepared activated carbon would be the main groups being significantly responsible for NH_3 adsorption capacity. This is because hydroxyl group of carboxylic and phenolic groups is able to interact with NH_3 via hydrogen bonding, either through the coordination of the nitrogen atom in the activating agent to the hydrogen of the hydroxyl group (OH/N) or the coordination of one of the three H atoms of NH_3 molecule to the oxygen of the hydroxyl group (NH/O) [33]. It can be concluded that the increase in the amount of strong acidic groups enhances NH_3 adsorption capacity. Mochizuki *et al.* [32] studied activated material derived from petcoke for NH_3 adsorption. It was observed that acidic functional groups, including hydroxyl phenolic, carboxylic and lactonic groups, mainly affect NH_3 adsorption efficiency. Furthermore, phenolic and carboxylic groups had higher determination coefficient of linearity value than lactonic group, indicating that both groups can be considered as major of all acidic surface groups to responsibly adsorb ammonia. The basis in an ammonia adsorption mechanism from acidic surface groups is the chemical interaction that acidic surface groups adsorb ammonia via hydrogen bonding, called chemisorption. This normally takes place at the active sites of the surface functional groups, which usually contain oxygen molecules [13]. Therefore, an increase in the amount of oxygen is represented in the form of acidic functional groups, resulting in enhancing chemisorption capacity.

From Table 5 and Figure 4, it can be indicated that the number of acidic surface groups are an important factor to determine the NH_3 adsorption efficiency of AC. Therefore, from the relationship between NH_3 adsorption capacity and the total acidic groups, AC13_500 shows the highest NH_3 adsorption capacity because of the highest total acidic groups and AC13_700 shows the lowest NH_3 adsorption capacity because of the lowest total acidic groups.

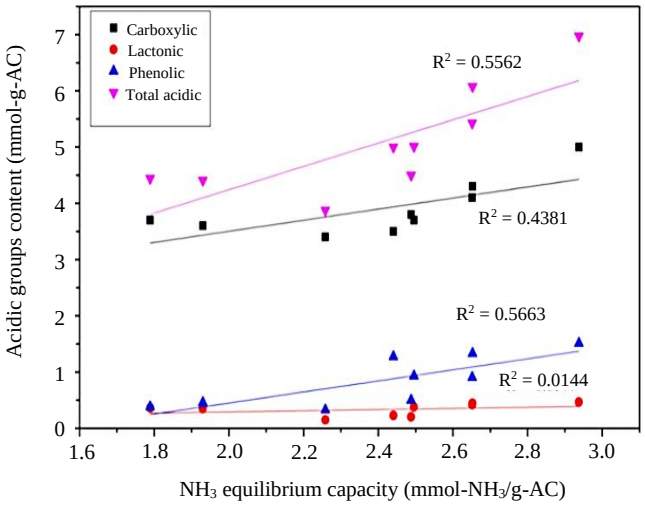

Figure 4. NH_3 equilibrium capacity as a function of acidic groups content of obtained AC.

In addition, Table 6 is exhibited hereon to compare NH_3 adsorption capacity and effectiveness of our obtained activated carbon with different adsorbents of other researchers who studied the impact of surface functional groups to ammonia adsorption.

3.6 Thermal properties of adsorptive PBS

The effect of activated carbon incorporated in PBS on thermal properties was evaluated by differential scanning calorimetry. In Figure 5(a), 2nd heating scan, first and second polymer melting temperature ($T_{m(1)}$ and $T_{m(2)}$) indicate that addition of activated carbon at 3 wt%, 6 wt%, 9 wt%, and 12 wt% has no significant difference to melting temperature of PBS when compared with neat PBS. In addition, $T_{m(1)}$ was presented at all thermograms of PBS with all AC contents. This can indicate that AC causes a significant change in crystal formation of PBS, resulting in development of more heterogeneous crystalline morphology. During the cooling scan, in Figure 5 (b), all thermograms display crystallization temperature (T_c) which shows that activated carbon addition is significantly affected crystallization temperature lower than neat PBS. This is probably due to the fact that activated carbon is able to act as a nucleating agent, leading to an increase in crystallization temperature during the cooling step [37].

To further clarify the thermal properties of PBS with activated carbon, Table 7 presents the $T_{m(1)}$, $T_{m(2)}$, T_c, $H_{m(1)}$, and $H_{m(2)}$ at various AC contents. The data confirms that $T_{m(2)}$ of PBS at all AC contents remains constant at 113°C, compared with neat PBS ($T_{m(2)}$ = 113.41°C). However, when focusing on the second enthalpy of melting ($H_{m(2)}$), this data is significantly lower with activated carbon addition of 3 wt%. The reason can be attributed to the bonding between its functional groups on the surface and polymer matrix, leading to hinder the chain arrangement of PBS and to decrease the crystallinity [38].

Table 6. Adsorption capacity of ammonia on different adsorbents.

Adsorbents	Total acidic functional groups (mmol/g-AC)	NH_3 adsorption capacity (mmol- NH_3/g-AC)	References
Nipa palm husk derived activated carbon	6.98	2.94	This work
Coconut shell-based activated carbon	2.06	2.42	[24]
Petroleum coke-based activated carbon	5.40	2.90	[32]
Treated lignite	3.78	2.21	[34]
Graphite oxide	2.705	0.91	[35]
Activated carbon fiber composites	2.91	1.35	[36]

Table 7. Thermal properties of all adsorptive PBS with various activated carbon content.

Sample	$T_{m(1)}$ (°C)	$T_{m(2)}$ (°C)	T_c (°C)	$H_{m(1)}$ ($J \cdot g^{-1}$)	$H_{m(2)}$ ($J \cdot g^{-1}$)
Neat PBS	102.87	113.41	81.50	-	72.43
PBS + 3 wt% AC	104.54	113.77	87.67	4.64	45.58
PBS + 6 wt% AC	103.94	113.48	87.67	4.39	51.82
PBS + 9 wt% AC	103.86	113.56	87.19	5.17	58.09
PBS + 12 wt% AC	104.48	113.71	87.63	4.88	48.89

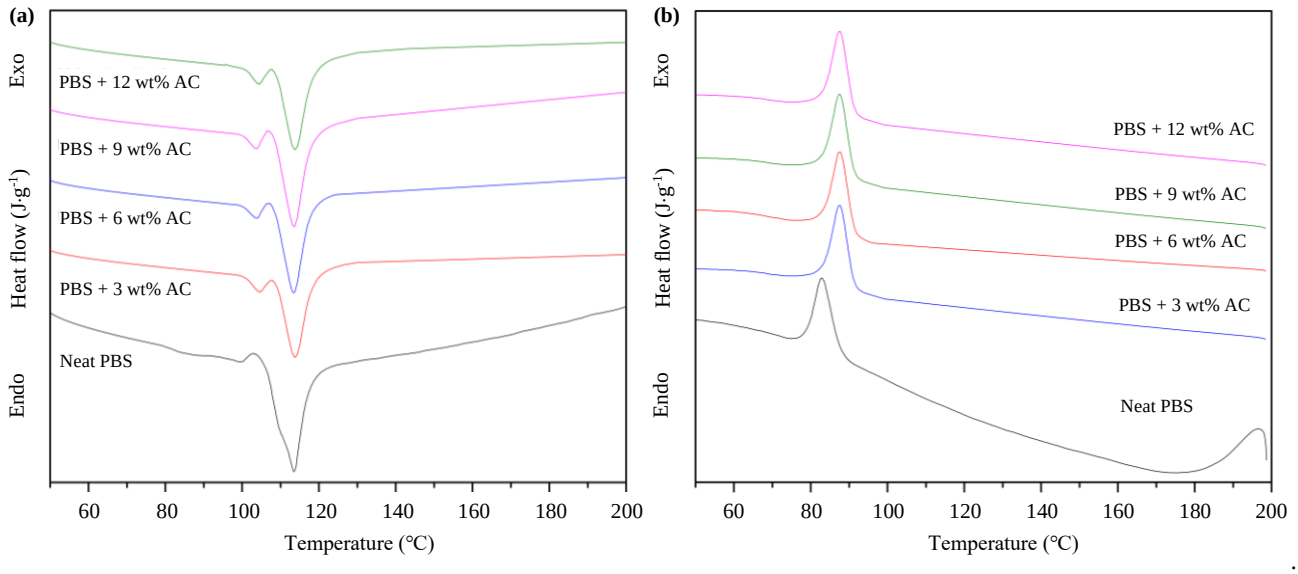

Figure 5. Differential scanning calorimetry thermograms of PBS with various activated carbon content (a) 2nd heating scan, and (b) cooling scan.

Interestingly, second melting enthalpy was continuously increased from 45.58 J·g^{-1} to 58.09 J·g^{-1} after addition of 3 wt% to 9 wt% activated carbon, respectively. It may be that activated carbon in PBS matrix can act as nucleating agent where crystal formation of PBS is easily induced, resulting in increased crystallinity. However, after 12 wt% of activated carbon incorporation with PBS, a significant decrease of melting enthalpy was obtained. This behavior can be explained that the agglomeration of activated carbon and non-uniform distribution took place, leading to stiffness in the structure due to steric hindrance from agglomerated AC. At high activated materials content, the proportion of PBS reduced, resulting in low crystallization phenomena.

3.7 FTIR spectroscopy of adsorptive PBS

FTIR characterization of surface functional groups of neat PBS and PBS with activated carbon is shown in Figure 6. FTIR spectra exhibited the characteristic band of neat PBS as stretching band at the region 2900 cm^{-1} to 2800 cm^{-1} represents -CH_2 peak, stretching of the carboxylic group (C=O) at around 1700 cm^{-1}, and stretching vibration of C-O bond at around 1049 cm^{-1}. After activated carbon addition, FTIR spectra significantly changed when compared with neat PBS at the region of 2900 cm^{-1} to 2800 cm^{-1}, 1700 cm^{-1}, and 1000 cm^{-1}. These regions are also characteristic peaks of AC13_500 which was previously described. Focusing on the region of 2900 cm^{-1} to 2800 cm^{-1}, a prominent peak was observed, representing the aliphatic CH_3 and CH_2 stretching. For peak around 1700 cm^{-1}, the spectrum of PBS with activated carbon slightly shifted, compared with neat PBS due to the existence of carbonyl group on the surface and interaction between AC and PBS matrix. According to Xiong *et al.*[39], they reported that the addition of 8 wt% activated carbon allowed carboxylic peak shifting from 1731 cm^{-1} to 1728 cm^{-1}. Furthermore, the peak intensity at the region of 1000 cm^{-1} decreased after 3 wt% AC addition. However, this peak intensity continuously increased with the increment of AC contents, indicating that C-O, -COO, and -OH groups of aromatic functional groups were better represented. In the same manner, the increase of activated carbon contents from 3 wt% to 12 wt% caused a simultaneous increase of these peak intensities from three regions. From this result, it can be concluded that the quantity of functional groups of AC on PBS-AC surface depends on the activated carbon contents. Here, PBS with 12 wt% AC provides the largest quantity of functional groups.

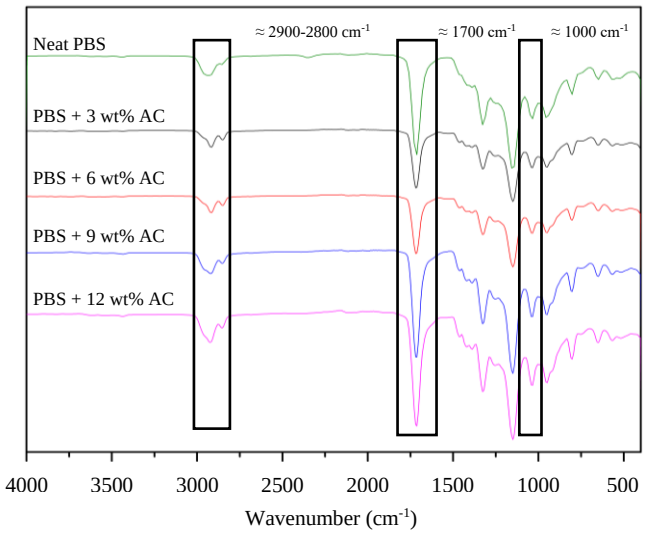

Figure 6. FTIR spectra of neat PBS and PBS with various activated carbon contents.

3.8 Wettability of adsorptive PBS

Contact angle is the method to indicate hydrophilic and hydrophobic characteristics during wettability testing [40]. contact angle is affected by interaction and intermolecular force between material surface and wetting liquid, which is referred to as significant factors [41]. In this study, neat PBS was also evaluated as a baseline case. Figure 7 displays the water contact angles on neat PBS and PBS with various activated carbon content. It was observed that neat PBS provided the highest contact angle about 90.16° ± 3.95°, indicating the lowest wettability or the highest hydrophobic characteristics among tested samples. In contrast, a decrease of contact angle was observed for PBS incorporated with activated carbon. The sequence orders of contact angle from high to low were PBS + 3 wt% AC (83.39° ± 2.31°), PBS + 6 wt% AC (79.68° ± 1.23°), PBS + 9 wt% AC (75.56° ± 2.82°) and PBS + 12 wt% AC (70.13° ± 3.28°). The result confirms that activated carbon addition improved the hydrophilicity of the surface. A similar finding was reported by Spahis *et al.* [42] that contact angle of PMMA and PS composites significantly decreased with increasing activated carbon loading in their polymer matrix.

From these results, one can be confirmed the existence of functional groups of activated carbon on the surface. Therefore, it can be explained that the chemistry of surface functional groups and interaction between surface and water can influence the decrease of contact angle. Following the FTIR result, the spectra of PBS with activated carbon show peaks involving these functional groups, C=O, C-O, and -OH, which were occurred on the surface. These polar functional groups could interact with the hydroxyl group of water molecules via hydrogen bonding, resulting in reduction of contact angle. Moreover, increase of AC contents led to the increment of polar functional groups which is definitely confirmed from continuous reduction of contact angle and observation of strong peak intensities of these polar groups.

3.9 Ammonia adsorption of adsorptive PBS

To study the effect of activated carbon addition to ammonia adsorption efficiency of prepared adsorptive PBS, neat PBS and PBS with different AC contents were placed in a plastic tube with ammonia gas of approximately 100 ppm to 110 ppm. After adsorption, NH_3 residue at the determined time was measured. Figure 8 shows the removal efficiency of studied samples. It can be seen from this figure that not only PBS with activated carbon could adsorb ammonia but also neat PBS since the latter still inherits polar functional groups such as carbonyl and hydroxyl groups, leading to interaction with ammonia molecule. Even though neat PBS could adsorb ammonia gas, adsorption data between neat PBS and PBS with AC is different. Comparing the effect of activated carbon contents, ammonia adsorption efficiency of PBS continuously improved with AC contents increased from 3 wt% to 12 wt%. Therefore, the highest ammonia

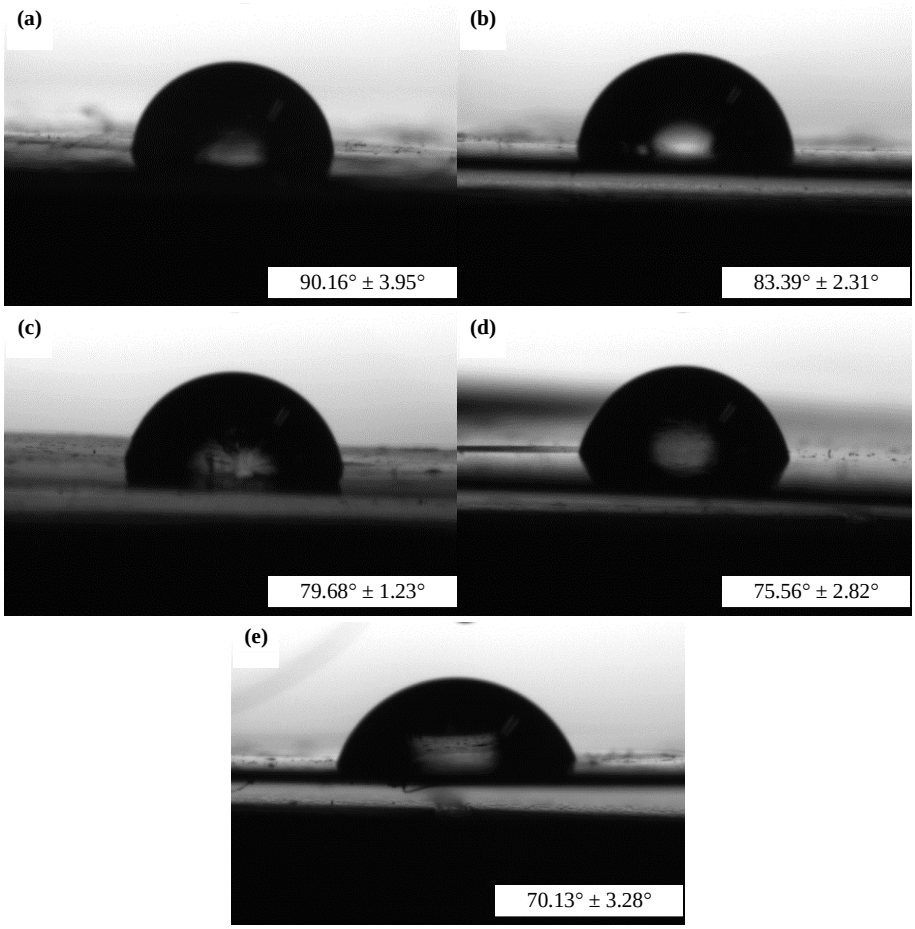

Figure 7. Water contact angle of (a) neat PBS and PBS with activated carbon, (b) 3 wt% AC, (c) 6 wt% AC, (d) 9 wt% AC, and (e) 12 wt% AC.

adsorption was observed at 12 wt% AC loading in which NH_3 was reduced to 24 wt% of the initial content (from 108 ppm to 26 ppm). The reason for this result can be explained following previous FTIR and contact angle results that more adsorption sites, referred to as C=O, C-O, and OH groups, were available with an increase in activated carbon content.

This result is consistent with a report of Long *et al*. [43] who observed ammonia concentration decreased with increasing prepared activated materials mass from 10 g to 40 g which suggested higher actual number of active sites. Adsorption behavior between activated carbon powder from the previous result and PBS with activated carbon was quite different. Adsorption by activated carbon powder was rapid within the first 1 h to 2 h, followed by slow removal when reaching an equilibrium state, while adsorption by PBS with activated carbon exhibited similar behavior at initial adsorption, even different behavior after 2 h. It can be seen that ammonia adsorption continuously took place beyond 2 h at slower adsorption but not reaching an equilibrium state. This phenomenon can be attributed that PBS sheet had lower surface area than activated carbon powder, which could provide less space to contact the ammonia molecule and functional groups on the surface [44]. Therefore, time was an important factor to obtain better ammonia adsorption performance. From Figure 8, it is observed that ammonia adsorption efficiencies of PBS with 12 wt% AC is slightly higher than PBS 9 wt% AC loading because, at higher activated carbon contents, agglomeration can occur which is confirmed from SEM that some functional groups interact with each other, resulting in reduction of free polar functional groups.

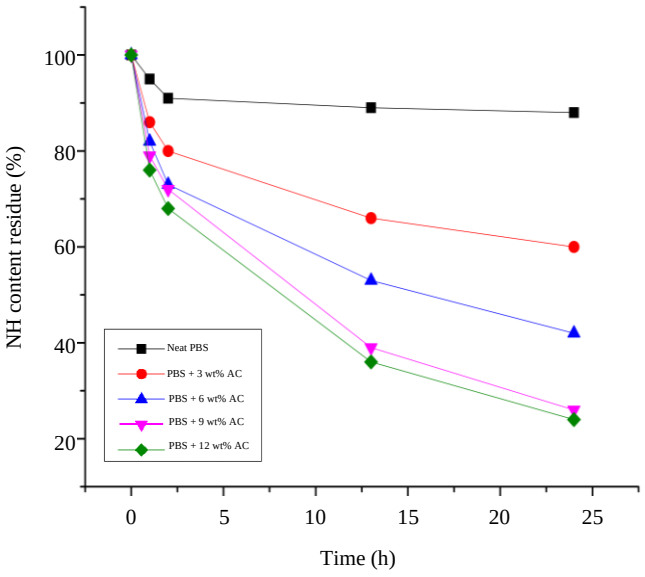

Figure 8. Removal efficiencies for NH_3 adsorbed on neat PBS and PBS with various activated carbon content within 24 h.

Table 8. Ammonia removal efficiency of different composites sorbents.

Composites	Experimental conditions	Amount adsorbed	References
PBS with 12 wt% AC	Concentration range: 100 mg·L^{-1} to 110 mg·L^{-1} Temperature: room temperature	76.00%	This work
Chitosan-coated micro-mesoporous zeolite	Concentration range: 50 mg·L^{-1} Temperature: 25°C	74.35%	[45]
Chitosan/Zeolite Y/Nano ZrO_2 nanocomposite	Concentration range: 20 mg·L^{-1} Temperature: 35°C	42.50%	[46]
Zirconium-based chitosan	Concentration range: 25 mg·L^{-1} to 30 mg·L^{-1} Temperature: 12°C	41.13%	[47]

From result being explained before in this part, it can be concluded that 12 wt% activated carbon was the optimum contents to incorporate with PBS to provide the optimal ammonia adsorption.

Furthermore, a comparison of adsorptive PBS and other composite sorbents on ammonia adsorption efficiency to display its superior performance is displayed in Table 8.

As a result of ammonia adsorption of adsorptive PBS, it can potentially be applied in practical application on various scales. Application of PBS adsorptive sheet in small scale, for example, can be utilized as adsorptive meat tray for ammonia adsorption. In fact, packaged fresh meat can continuously generate ammonia due to deteriorating meat protein by spoilage bacteria on its surface. If ammonia is accumulated to a high level in packaging, it will be harmful to human health accompanied by the terrible odor and undesirable flavor of meat [48]. Hence, our adsorptive PBS in the form of a tray can alleviate this pain point by adsorbing ammonia from meat, leading to extended shelf-life of meat. Adsorptive PBS can be utilized not only in small scale applications but also on large scale agricultural operations. As disclosed in the manuscript, ammonia is an important hazardous pollutant, being seriously harmful to human health. Surprisingly, agriculture activity is the greatest contributor of ammonia to the earth's atmosphere [49]. The sequential order of agriculture activity includes livestock manure, use of natural fertilizers, and mineral nitrogen fertilizers [50]. Therefore, this adsorptive PBS can be installed as filter sheets at the back of an exhaust fan in livestock buildings or in the greenhouse to filter ammonia from these activities, before discharging to the environment. Moreover, it could be buried to adsorb ammonia released from fertilizer in the soil.

4. Conclusions

Activated carbon from Nipa palm husk was successfully prepared via KOH chemical activation. NH_3 adsorption capability of AC mainly depends on the preparation condition. The optimum condition of activated material with the highest adsorption value within 24 h was through pretreatment of the raw material with KOH at an impregnation ratio of 1:3 and then activated at 500°C. The high adsorption capability of prepared AC depends mainly on acidic groups content on carbon surface, especially phenolic and carboxylic group which was found to be approximately linear in proportion with NH_3 adsorption equilibrium. The amount of acidic content increased with decreasing impregnation ratio at low activation temperature. However, surface area and total pore volume were not directly relative to NH_3 adsorption capacity.

The optimum activated carbon contents to provide the greatest ammonia adsorption of the adsorptive PBS was 12 wt% due to the highest acidic functional groups displayed on PBS surface. However, higher acidic groups on PBS surface led to the reduction of water contact angle, and crystallinity.

Prepared activated carbon from Nipa palm husk exhibits strong potential as quality functional porous carbon for an alternative source of cheap and naturally renewable raw material. In addition to added value of this material, this would be a sustainable solution in place of imported AC obtained from wood. Furthermore, it can be mixed with PBS to fabricate adsorptive PBS sheet which can be applied in livestock and fertilizer industry since these industries have emitted the large amount of ammonia.

Acknowledgements

This work was supported by doctoral scholarship of the 100th Anniversary Chulalongkorn University for financial support.

References

[1] N. F. Attia, M. A. Diab, A. S. Attia, and M. F. El-Shahat, "Greener approach for fabrication of antibacterial graphene-polypyrrole nanoparticle adsorbent for removal of Mn^{2+} from aqueous solution," *Synthetic Metals*, vol. 282, p. 116951, 2021.

[2] A. Galal, M. M. Zaki, N. F. Atta, S. H. Samaha, H. E. Nasr, and N. F. Attia, "Electroremoval of copper ions from aqueous solutions using chemically synthesized polypyrrole on polyester fabrics," *Journal of Water Process Engineering*, vol. 43, p. 102287, 2021.

[3] J. Park, S. Y. Cho, M. Jung, K. Lee, Y. C. Nah, N. F. Attia, and H. Oh, "Efficient synthetic approach for nanoporous adsorbents capable of pre- and post-combustion CO_2," *Journal of CO_2 Utilization*, vol. 45, p. 101404, 2021.

[4] M. A. Diab, N. F. Attia, A. S. Attia, and M. F. El-Shahat, "Green synthesis of cost-effective and efficient nanoadsorbents based on zero and two dimensional nanomaterials Zn^{2+} and Cr^{3+} removal from aqueous solutions," *Synthetic Metals*, vol. 265, p. 116411, 2020.

[5] J. Park, T. Kang, Y. Heo, K. Lee, K. Kim, K. Lee, and C. Yoon, "Evaluation of short-term exposure levels on ammonia and hydrogen sulfide during manure-handling processes at livestock farms," *Safety and Health at Work*, vol. 11, pp. 109-117, 2020.

[6] M. A. Farea, H. Y. Mohammed, S. M. Shirsat, P. W. Sayyad, N. N. Ingle, T. Al-Gahouari, M. M. Mahadik, G. A. Bodkhe, and M. D. Shirsat, "Hazardous gases sensors based on conducting polymer composites: Review," *Chemical Physics Letters*, vol. 776, p. 138703, 2021.

[7] S. J. Blonigen, A. G. Fassbender, R. D. Litt, B. F. Monzyk, and R. Neff, "Apparatus and method for ammonia removal from waste streams," *U.S. patent 6,838,069*, published Jan 4, 2005.

[8] M. Danish, R. Hashim, M. N. M. Ibrahim, and O. Sulaiman, "Effect of acidic activating agents on area and surface functional groups of activated carbons produced from *Acacia mangium* wood**,**" *Journal of Anaytical and Applied Pyrolysis*, vol. 104, pp. 418-425, 2013.

[9] X. Wang, H. Cheng, G. Ye, J. Fan, F. Yao, Y. Wang, Y. Jiao, W. Zhu, H. Huang, and D. Ye, "Key factors and primary modification methods of activated carbon and their application in adsorption of carbon-based gases: A review," *Chemosphere*, vol. 287, no. 2, p. 131995, pp. 1-19, 2022.

[10] C. A. Toles, W. E. Marshall, and M. M. Johns, "Surface functional groups on acid-activated nutshell carbons," *Carbon*, vol. 37, pp. 1207, 1999.

[11] B. J. Kim, and S. J. Park, "Effects of carbonyl group formation on ammonia adsorption of porous carbon surfaces," *Journal of Colloid and Interface Science*, vol. 311, pp. 311-314, 2007.

[12] J. Guo, W. S. Xu, Y. L. Chen, and A.C. Lua, "Adsorption of NH_3 onto activated carbon prepared from palm shells impregnated with H_2SO_4," *Journal of Colloid and Interface Science*, vol. 281, pp. 285-290, 2005.

[13] A. J. Allen, L.Whitten, and G. Mckay, "The production and characterization of activared carbons: A review," *Developments in Chemical Engineering and Mineral Process*, vol. 6, pp. 2311-261, 1988.

[14] S. Kim, S. Y. Cho, K. Son, N. F. Attia, and H. Oh, "A metal-doped flexible porous carbon cloth for enhanced CO_2/CH_4 separation," *Separation and Purification Technology*, vol. 227, p. 119511, 2021.

[15] M. Jung, J. Park, S. Y. Cho, S. E. A. Elashery, N. F. Attia, and H. Oh, "Flexible carbon sieve based on nanoporous carbon cloth for efficient CO_2/CH_4 separation," *Surfaces and Interfaces* vol. 23, p. 100960, 2021.

[16] M. Jung, J. Park, K. Lee, N. F. Attia, and H. Oh, "Effective synthesis route of renewable nanoporous carbon adsorbent for high energy storage and CO_2/N_2 selectivity," *Renewable Energy*, vol.161, pp. 30-42, 2020.

[17] A. Demirbas, "Agricultural based activated carbons for the removal of dyes from aqueous solutions: A review," *Journal of Hazardous Materials*, vol. 167, pp. 1-9, 2009.

[18] D. Sud, G. Mahajan, and M. P. Kaur, "Agricultural waste material as potential adsorbent for sequestering heavy metal ions from aqueous solutions-A review," *Bioresource Technology*, vol. 99, pp. 6017-6027, 2008.

[19] M. *Baysal*, K. *Bilge*, B. *Yılmaz*, M. *Papila*, and Y. *Yürüm*, "Preparation of high surface area activated carbon from waste-biomass of sunflower piths: Kinetics and equilibrium studies on the dye removal**,**" Journal of Environmental Chemical Engineering, vol. 6, issue 2, pp. 1702-1713, 2018.

[20] P. Tamunaidu, and S. Saka, "Chemical characterization of various parts of nipa palm (Nypa fruticans)," *Industrial Crops and Products*, vol. 34, no. 3, pp. 1423-1428, 2011.

[21] V. Sricharoenchaikul, C. pechyen, D. Aht-ong, and D. Atong, "Preparation and characterization of activated carbon from the pyrolysis of physic nut (*Jatropha curcus L.*)," *Energy and Fuels*, vol. 22, no. 1, pp. 31-37, 2008.

[22] S. Brunauer, S. Emmett, and F. Teller, "Adsorption of gases in multimolecular layers," *Journal of the American Chemical Society*, vol. 60, pp. 309-319, 1951.

[23] H. P. Boehm, "Some aspects of the surface chemistry of carbon blacks and other carbons," *Carbon*, vol. 32, pp. 759-769, 1994.

[24] C. C. Huang, H. S. Li, C. H. Chen, "Effect of surface acidic oxides of activated carbon on of ammonia," *Journal of Hazardous Materials*, vol. 159, pp. 523-527, 2008.

[25] X. Jin, Z. Yu, and Y. U.Wu, "Preparation of activated carbon from lignin obtained by straw pulping by KOH and K_2CO_3," *Cellulose Chemistry and Technology*, vol. 46, pp. 79-85, 2012.

[26] R. L. Tseng, S. K. Tseng, F. C. Wu, C. C. Hu, and C. C. Wang, "Effects of micropore development on the physicochemical properties of KOH-activated carbons," *Journal of the Chinese Institute of Chemical Engineers*, vol. 39, no. 1, pp. 37-47, 2008.

[27] S. Mopoung, P. Moonsiri, W. Palas, and S. Khumpai, "Characterization and properties of activated carbon prepared from tarmarind seeds by KOH activation for Fe(III) adsorption from aqueous solution," *The Scientific World Journal*, 2015.

[28] A. García-García, A. Gregório, C. Franco, F. Pinto, D. Boavida, and I. Gulyurtlu, "Unconverted chars obtained during biomass gasification on a pilot scale gasifier as a source of activated carbon production**,**" *Bioresource Technology*, vol. 88, pp. 27-32, 2003.

[29] S. J. Park, and W. Y. Jung, "Preparation and structural characterization of activated carbons based on polymeric resin**,**" *Journal of Colloid and Interface Science*, vol. 250, pp. 196-200, 2002.

[30] K. L. Van, and T. T. L. Thi, "Activated carbon derived from rice husk by NaOH activation and its application in supercapacitor**,**" *Progress in Natural Science: Materials International*, vol. 24, pp. 191-198, 2014.

[31] J. L. Figueiredo, M. F. R. Pereira, M. M. A. Freitas, and J. J. M. Orfao, "Modifications of the surface chemistry of activated carbons**,**" *Carbon*, vol. 37, pp. 1379-1389, 1999.

[32] T. Mochizuki, M. Kubota, H. Matsuda, and L. F. D'Elia Camacho, "Adsorption behaviors of ammonia and hydrogen sulfide on activated carbon prepared from petroleum coke by KOH chemical activation**,"** *Fuel Processing Technology*, vol. 144, pp. 164-169, 2016.

[33] N. A. Travlou, M. Seredych, E. Rodriguez-Castellon, and T. J. Bandosz, "Activated carbon-based gas sensors: effects of surface features on the sensing mechanism**,**" *Journal of Materials A*, vol. 3, pp. 3821-3831, 2015.

[34] B. Han, W. zhang, J. Z. He, and D. Chen, "Lignite ammonia adsorption and surface chemistry after dewatering," *Separation and Purification Technology*, vol. 253, 117483, 2020.

[35] M. Seredych, and T. J. Bandosz, "Mechanism of ammonia retention on graphite oxides: Role of surface chemistry and

structure," *The Journal of Physical Chemistry C*, vol. 111, pp. 15596-15604, 2007.

[36] W. Zheng, J. Hu, S. Rappeport, Z. Zheng, Z. Wang, Z. Han, J. Langer, and J. Economy, "Activated carbon fiber composites for gas phase ammonia adsorption," *Microporous and Mesoporous*, vol. 234, pp. 146-154, 2016.

[37] Y. Gao, O. T. Picot, H. Zhang, E. Bilotti, and T. Peus, "Synergistic effects of filler size on thermal annealing-induced percolation in polylactic acid (PLA/Graphite nanoplatelet (GNP nanocomposites," *Nanocomposites*, vol. 3, no. 2, pp. 67-75, 2017.

[38] M. El. Achaby, F. E. Arrakhiz, S. Vaudreuil, Q. El Kacem, M. A. Bousmina, and O. Fassi-Fehri, "Mechanical, thermal, and rheological properties of graphene-based polypropylene nanocomposites prepared by melt mixing," *Polymer Composites*, vol. 33, pp. 733-744, 2012.

[39] L. W. Xiong, and K. H. Badri, "Preparation of polyurethane composited with activated carbon z black as the reinforcing filler," *Journal of Polymer Science and Technology*, vol. 3, no. 1, pp. 11-18, 2018.

[40] M. A. Herrera, A. P. Mathew, and K. Oksman, "Gas permeability and selectivity of cellulose nanocrystals films(layers) deposited by spin coating," *Carbohydrate. Polymer*, vol. 112, pp. 494-501, 2014.

[41] R. David, and A. W. Neumann, "A theory for surface tensions and contact angles of hydrogen-bonding liquids," *Langmuir*, vol. 30, no. 39, pp. 11634-11639, 2014.

[42] N. Spahis, M. Dellali, and H. Mahmoudi, "Synthesis and characterization of polymeric/activated carbon membranes," *Procedia Engineering*, vol. 33, pp. 47-51, 2012.

[43] X. L. Long, H. Cheng, X. L. Xin, W. D. Xiao, W. Li, and W. K. Yuan, "Adsorption of ammonia on activated carbon form aqueous solutions," *Environmental Progress*, vol. 27, no. 2, pp. 225-233, 2008.

[44] M. Anson, J. Marchese, E. Garis, N. Ochoa, and C. Pagliero, "ABS copolymer-activated carbon mixed matrix membranes for CO_2/CH_4 seperation," Journal of Membrane Science, vol. 243, pp. 19-28, 2004.

[45] Y. G. Guo, Y. Zhao, and Y. J. Guo, "Removal of ammonia-nitrogen in wastewater by chitosan-coated micro-mesoporous zeolite," *Chinese Journal of Environmental Engineering*, vol. 9, pp. 2067-2072, 2015.

[46] A. Teimouri, S. G. Nasab, and N. Vahdatpoor, "Chitosan/ Zeolite Y /Nano ZrO_2 nanocomposite as an adsorbent for the removal of nitrate from the aqueous solution," *International Journal of Biological Macromolecules*, vol. 93, pp. 254-266, 2016.

[47] M. Q. Sun, Y. N. Gao, and L. T. Zhou, "Study on optimization of modified chitosan for removal of nitrate by response surface methodology," *Environmental Engineering*, vol. 36, pp. 33-37, 2018.

[48] C. Hagyard, T. Cummings, and A. Martin, "Effect of ammonia exposure on subsequent rancid flavor development in lamp," *Journal of Muscle Food*, vol. 4, no. 3, pp. 254-251, 1993.

[49] A. Faber, Z, Jarosz, and T. Zylowski, "Verification of the possibilities to reduce ammonia emission for various slurry application practice in Poland," *Problems of World Agriculture*, vol, 19, pp. 31-40, 2019.

[50] A. Sapek, "Emission of ammonia from agriculture in Poland," *Zagadnienia Ekonomiki Rolnej*, vol. 2, pp. 114-123, 2013.